CHAPTER VIII

Thermophysical properties of the binary mixtures of cyclohexanone with some esters

8.1. Introduction

The study of molecular interactions in binary and multi-component liquid mixtures is of significant importance and interest to both chemists and chemical engineers in view of their diversified applications. A knowledge of excess functions like excess molar volume, excess isentropic compressibility, *etc.*, may help to interpret, correlate and even predict thermodynamic properties of liquid mixtures as well as simulate their liquid state in order to design new industrial process equipments with better precision at reduced costs and hence such knowledge is an avenue for the study of molecular interactions in terms of structural effects and packing phenomenon.[1-4] Thus systematic investigation on the different physico-chemical properties (volumetric, viscometric and acoustic, *etc*.) and their excess/deviation functions are of great importance in chemical industry. Therefore herein this chapter an attempt has been undertaken to study the nature of molecular interactions in the binary mixtures of cyclohexanone (CHN) with some esters, *viz.*, methyl acetate (MA), ethyl acetate (EA) and methyl salicylate (MS) at 298.15, 308.15 and 318.15 K under ambient pressure. In chapter VII the thermophysical properties of the binary mixtures of cyclohexane with these esters were studied. The selected liquids were chosen due to their varied applications. Cyclohexanone is used as an intermediate in nylon manufacture and as a solvent for natural resins, lacquers, dyes and insecticides, *etc*. Esters are also industrially important liquids because of their wide usage in flavoring, perfumery, artificial essences and cosmetics, *etc*., as mentioned in chapter VII.

Herein this chapter experimental data (ρ, η, u and n_D) were used to determine different excess or deviation functions and are discussed in terms of molecular interactions, structural effects and the nature of liquid mixtures. Again a quantitative estimation of different contributions (*i.e.*, interaction contribution, free volume contribution, *etc*.) to the excess molar volumes (V_m^E) of the binary mixtures at ambient temperature and pressure were determined from PFP theory.[5,6] A comparison was also made between the experimental and calculated V_m^E and η values (based on PFP[5] or Bloomfield-Dewan viscosity model[7] and PREOS[8]) to assess the predictive capability

of these theories. Furthermore, ultrasonic speeds of sound and refractive indices for all the binary mixtures were theoretically predicted based on several empirical and semi-empirical relations.

8.2. Experimental section

8.2.1. *Materials*

All the chemicals used in this chapter were of spectroscopic grade (Sigma-Aldrich, Germany, Reagent Plus, purity > 99%) and were used as received from the vendor. A comparison between the experimental and literature density and viscosity data of the selected esters at the experimental temperatures and pressure has been shown in the previous chapter and such a comparison between the experimental and literature density and viscosity data[9-12] of cyclohexanone has been given in Table 8.1 for ascertaining its purity.

8.2.2. *Apparatus and procedures*

All the binary mixtures were prepared afresh by mass before use inside a dry box by mass at 298.15 K and kept in air-tight bottles with stopper. Each prepared solution was distributed into three recipients to perform all the measurements in triplicate. The mass measurements were recorded on a digital electronic analytical balance (Mettler, AG 285, Switzerland) with an uncertainty of ±0.01 mg. The uncertainty in mole fraction was evaluated to be ±0.0002. Densities (ρ) were measured with a vibrating-tube densitometer (Anton Paar, DMA 4500M). Viscosities (η) were measured by means of a suspended Canon-type Ubbelhode viscometer, thoroughly cleaned, dried and placed vertically in a glass sided thermostat maintained to ±0.01 K of the desired temperature. Ultrasonic speeds of sound (u) were measured with a multi-frequency ultrasonic interferometer (F-05, Mittal Enterprises, New Delhi, India) working at 2 MHz. Refractive indices of pure liquid and their binary mixtures were measured with an Abbe's refractometer. The details of the instruments, their calibrations and uncertainties of the measured properties are given in chapter III.

8.3. Results and discussion

Excess or deviation functions are sensitive to the nature and degree of the intermolecular forces operating amongst the unlike and like components in the liquid mixtures. Therefore, the systematic investigation of the excess or deviation functions

Table 8.1. Densities (ρ) and viscosities (η) of the pure liquids at T = (298.15-318.15) K

Pure Liquid	T (K)	$\rho \cdot 10^{-3}$ (kg · m^{-3})		η (mPa · s)	
		Expt.	Lit.	Expt.	Lit.
CHN	298.15	0.94165	0.9416[9] 0.9418[10]	2.021	0.020[9] 2.0205[10]
	308.15	0.93128	0.9312[11]	1.656	1.6562[11]
	318.15	0.92346	0.9234[11]	1.381	1.3809[11]
	318.15	1.15942	1.159405[12]	1.303	

for the liquid mixtures (differing in size, shape and polarity, *etc*.) is the initial step for a fundamental understanding of the physico-chemical behavior and the nature of the molecular interactions amongst the unlike molecules in the mixtures. The sign and magnitude of these excess or deviation functions depend upon the relative magnitude of contractive and expansive factors that arise on mutual mixing of the components and often give a measure of non-ideality in the liquid mixtures involved. The experimental values of densities (ρ), viscosities (η), excess molar volumes (V_m^E) and viscosity deviation ($\Delta\eta$) of the binary mixtures under investigation as a function of mole fraction (x_1) of CHN at the experimental temperatures are listed in Table 8.2.

8.3.1. *Excess molar volumes*

Excess molar volume (V_m^E) reflects the overall state of the packing effects, molecular arrangements and interactions prevailing amongst the components of the binary mixtures and arises as a result of several effects or contributions, *viz.*, physical, chemical and geometrical contribution. The physical contributions (like breaking of liquid order on mutual mixing) mainly involve the dispersion forces, non-specific and unfavorable interactions amongst the unlike components in the mixtures. The chemical or specific interactions involve hydrogen bond formation, dipole-dipole or dipole-induced dipole interactions, charge transfer type forces and other complex forming interactions amongst dissimilar species. Structural contributions arise from the differences in molecular packing due to interstitial accommodation of one component into other's structure provided the components differ in size, shape and volume. While physical contributions cause volume expansion (*i.e.*, positive V_m^E), chemical and geometrical contributions cause volume contraction (*i.e.*, negative V_m^E).

Using the measured densities of the mixtures, excess molar volumes (V_m^E) were obtained from the relation:

$$V_m^E = \sum_{i=1}^{2} x_i M_i (1/\rho - 1/\rho_i) \qquad (1)$$

where ρ is the density of the mixture and x_i, M_i and ρ_i are the mole fraction, molar mass and density of the i^{th} component in a mixture, respectively. The uncertainty in the excess molar volumes (V_m^E) was evaluated to be ±0.006 $cm^3 \cdot mol^{-1}$. Figure 8.1 (V_m^E *versus* x_1 at 298.15 K) illustrate that excess molar volumes (V_m^E) vary in a sigmoid fashion with mole fraction (x_1) of CHN for the binary mixtures with the alkyl esters (MA and EA) at 298.15 K. Similar composition dependence of V_m^E values was observed at other experimental temperatures. The V_m^E values are positive at the lower mole fraction (x_1) of CHN and become negative at the mole fractions $x_1 \geq 0.6378$ and $x_1 \geq 0.4730$ for the mixtures (CHN + MA) and (CHN + EA), respectively but for the mixture (CHN + MS) the V_m^E values are negative over the entire composition range at all the experimental temperatures. Almost similar results were reported earlier for the mixtures with alkyl esters at 298.15 K by Roy *et al.*[9] CHN is a polar associated liquid through dipole-dipole interactions and esters also exist as dipolar associates. So an approximate estimate of the nature and strength of molecular interactions between similar or dissimilar molecules can be guessed from their dipole moments (μ_D). The ascending order of the dipole moment (μ_D) of the selected liquids is: $\mu_{D,\,MA}$ (1.72) < $\mu_{D,\,EA}$ (1.78) < $\mu_{D,\,MS}$ (2.47) < $\mu_{D,\,CHN}$ (2.87) in Debye.[13] A comparison of the dipole moments (μ_D) reveals that the intermolecular interactions should be lowest in the mixture (CHN + MA) and highest in the mixture (CHN + MS) and the expected order of molecular interactions amongst the unlike components in the mixtures should be (CHN + MS) > (CHN + EA) > (CHN + MA) based on the degree of dipole-dipole interactions. The observed positive variation of V_m^E values for the mixtures (CHN + MA) and (CHN + EA) with mole fraction (x_1) of CHN is due to the breaking of dipole-dipole cohesive forces present amongst the similar molecules on mutual mixing of the dissimilar molecules.

Table 8.2. Density (ρ), viscosity (η), excess molar volume (V_m^E) and viscosity deviation ($\Delta\eta$) for the binary mixtures studied at T = (298.15 to 318.15) K.

x_1	$\rho \cdot 10^{-3}$ (kg·m^{-3})	η (mPa·s)	$V_m^E \cdot 10^6$ (m^3·mol^{-1})	$\Delta\eta$ (mPa·s)
CHN (1) + MA (2)				
T = 298.15 K				
0	0.92681	0.3810	0	0
0.0774	0.92744	0.3952	0.0735	-0.038
0.1587	0.92858	0.4262	0.1047	-0.070
0.2444	0.92995	0.4834	0.1166	-0.089
0.3347	0.93149	0.5647	0.1134	-0.101
0.4301	0.93314	0.6797	0.0999	-0.101
0.5310	0.93522	0.8284	0.0434	-0.095
0.6378	0.93729	1.0332	-0.0144	-0.071
0.7512	0.93917	1.2861	-0.0550	-0.048
0.8717	0.94072	1.6093	-0.0618	-0.022
1	0.94165	2.0209	0	0
T = 308.15 K				
0	0.91524	0.3491	0	0
0.0774	0.91598	0.3429	0.0759	-0.051
0.1587	0.91713	0.3449	0.1178	-0.102
0.2444	0.91856	0.3668	0.1357	-0.144
0.3347	0.92014	0.4167	0.1404	-0.171
0.4301	0.92193	0.5197	0.1250	-0.162
0.5310	0.92409	0.6539	0.0719	-0.144
0.6378	0.92631	0.8255	0.0103	-0.117
0.7512	0.92828	1.0483	-0.0271	-0.076
0.8717	0.92992	1.3266	-0.0296	-0.030
1	0.93128	1.6564	0	0
T = 318.15 K				
0	0.90225	0.3132	0	0
0.0774	0.90320	0.2682	0.1048	-0.083
0.1587	0.90488	0.2551	0.1457	-0.141
0.2444	0.90674	0.2679	0.1718	-0.182
0.3347	0.90890	0.3083	0.1703	-0.206
0.4301	0.91119	0.3907	0.1565	-0.202
0.5310	0.91380	0.5101	0.1099	-0.178
0.6378	0.91643	0.6546	0.0599	-0.152
0.7512	0.91908	0.8514	0.0064	-0.103
0.8717	0.92146	1.0971	-0.0186	-0.044
1	0.92346	1.3807	0	0
CHN (1) + EA (2)				
T = 298.15 K				
0	0.89455	0.4262	0	0
0.0907	0.89863	0.4607	0.0459	-0.030
0.1833	0.90306	0.5139	0.0584	-0.053
0.2778	0.90769	0.5924	0.0536	-0.064
0.3744	0.91256	0.6973	0.0279	-0.066
0.4730	0.91754	0.8297	-0.0051	-0.060

0.5738	0.92293	0.9920	-0.0778	-0.049
0.6769	0.92798	1.1849	-0.1076	-0.037
0.7822	0.93298	1.4117	-0.1260	-0.028
0.8899	0.93759	1.6884	-0.0962	-0.014
1	0.94165	2.0209	0	0
		T = 308.15 K		
0	0.88267	0.3875	0	0
0.0907	0.88663	0.3971	0.0760	-0.045
0.1833	0.89104	0.4367	0.1066	-0.069
0.2778	0.89581	0.4971	0.1018	-0.083
0.3744	0.90088	0.5829	0.0692	-0.085
0.4730	0.90602	0.6939	0.0341	-0.076
0.5738	0.91137	0.8286	-0.0186	-0.063
0.6769	0.91662	0.9866	-0.0541	-0.049
0.7822	0.92170	1.1760	-0.0638	-0.031
0.8899	0.92664	1.3920	-0.0519	-0.020
1	0.93128	1.6564	0	0
		T = 318.15 K		
0	0.86994	0.3564	0	0
0.0907	0.87415	0.3451	0.1002	-0.058
0.1833	0.87892	0.3678	0.1421	-0.089
0.2778	0.88413	0.4180	0.1395	-0.101
0.3744	0.88972	0.4938	0.1004	-0.098
0.4730	0.89521	0.5874	0.0798	-0.089
0.5738	0.90111	0.6972	0.0195	-0.078
0.6769	0.90703	0.8321	-0.0356	-0.059
0.7822	0.91261	0.9932	-0.0430	-0.035
0.8899	0.91812	1.1654	-0.0351	-0.024
1	0.92346	1.3807	0	0
		CHN (1) + MS (2)		
		T = 298.15 K		
0	1.17931	1.5358	0	0
0.1469	1.15497	1.6132	-0.5092	0.014
0.2793	1.13044	1.6852	-0.8422	0.027
0.3992	1.10597	1.7545	-1.0413	0.041
0.5082	1.08166	1.8141	-1.1289	0.048
0.6079	1.05751	1.8639	-1.1147	0.049
0.6993	1.03357	1.906	-1.0112	0.045
0.7834	1.00995	1.9394	-0.8366	0.035
0.8611	0.98676	1.9695	-0.6069	0.024
0.9331	0.96381	1.9962	-0.3069	0.012
1	0.94165	2.0209	0	0
		T = 308.15 K		
0	1.16931	1.4024	0	0
0.1469	1.14342	1.4484	-0.3597	0.011
0.2793	1.11840	1.4912	0.6562	0.022
0.3992	1.09389	1.5296	-0.8635	0.031
0.5082	1.06923	1.5609	-0.9211	0.035
0.6079	1.04518	1.5854	-0.9218	0.034
0.6993	1.02094	1.6047	-0.7855	0.029
0.7834	0.99744	1.6199	-0.6207	0.022
0.8611	0.97477	1.6330	-0.4426	0.014
0.9331	0.95299	1.6454	-0.2650	0.007

1	0.93128	1.6564	0	0
		T = 318.15 K		
0	1.15942	1.3027	0	0
0.1469	1.13269	1.3210	-0.2428	0.007
0.2793	1.10771	1.3403	-0.5227	0.016
0.3992	1.08335	1.3565	-0.7252	0.023
0.5082	1.05892	1.3682	-0.7849	0.026
0.6079	1.03477	1.3753	-0.7510	0.026
0.6993	1.01120	1.3789	-0.6641	0.022
0.7834	0.98801	1.3806	-0.5092	0.017
0.8611	0.96552	1.3802	-0.3269	0.011
0.9331	0.94431	1.3796	-0.1905	0.004
1	0.92346	1.3807	0	0

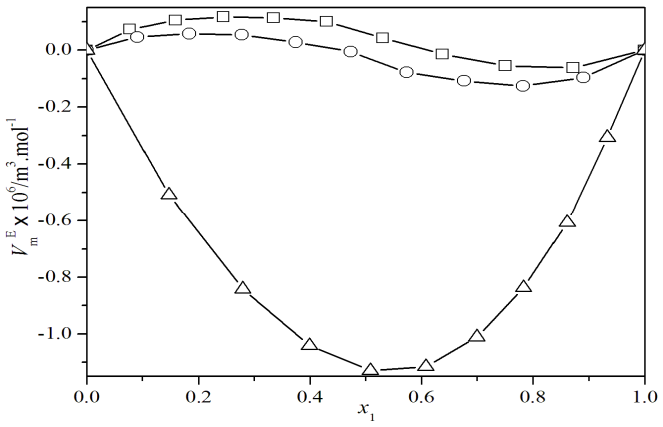

Fig. 8.1. Excess molar volume (V_m^E) *versus* mole fraction of CHN (x_1) for the binary mixtures of CHN with some esters at T = 298.15 K. The graphical points represent excess molar volumes (V_m^E) for the mixtures with: □, MA; ○, EA; Δ, MS.

At dilute to moderate CHN region V_m^E values augment with increasing mole fraction (x_1) of CHN for the mixtures (CHN + MA) and (CHN + EA) indicating that free volumes amongst the unlike molecules are increasing due to loose packing of the component molecules in the mixtures. This effect is maximum at $x_1 \approx 0.2444$ and $x_1 \approx 0.1833$ for the mixtures (CHN + MA) and (CHN + EA), respectively. However at CHN rich region V_m^E values decrease and become negative for the mixtures (CHN + MA) and (CHN + EA). Hence there is increase in the compactness of the liquid structure due to close packing. This close packing or compactness in the liquid structure may be attributed to: (i) the interstitial accommodation or the geometrical fitting of the ester molecules in the free space or vacancies between the CHN

molecules or *vice-versa*, (ii) the dipole-dipole interactions amongst the CHN and the ester molecules and iii) intermolecular hydrogen bond interactions. Furthermore it is seen that although both the mixtures (CHN + MA) and (CHN + EA) follow the similar trend in V_m^E values, the interactions amongst the unlike components in the mixture (CHN + EA) is more compared to those in the mixture (CHN + MA). This may be due to more polar nature of EA compared to that of MA and greater dipole-dipole interactions in the mixture (CHN + EA). On the contrary the V_m^E values for the mixture (CHN + MS) are negative over the entire composition range at all the experimental temperatures. MS is self-associated through dipolar interactions as well as intramolecular hydrogen bonding and the mixing of CHN with MS perturbs the self-associated structure of MS and induce specific hydrogen bond interactions between the -OH group of MS and >C=O group of CHN molecules in the mixture (CHN + MS), strong dipole-dipole interactions as well as interstitial accommodation of CHN molecules in the free space between MS molecules ($V_{m,MS} - V_{m,CHN}$ = 24.79 $cm^3 \cdot mol^{-1}$ at 298.15 K). These effects ultimately increase the intermolecular compactness in this mixture ultimately leading to volume contraction. Therefore, the molecular interactions in the studied binaries follow the order: (CHN + MS) > (CHN + EA) > (CHN + MA). Furthermore, V_m^E values for all the studied mixtures increase with a rise in the experimental temperature from 298.15 to 318.15 K over the entire composition range. Such a temperature dependence of V_m^E values suggests that temperature enhancement reduces or disturbs developing specific and non-specific interactions amongst the component molecules due to thermal agitation.

The partial molar volumes ($\overline{V}_{m,i}$) of the i^{th} component in the mixtures were obtained at 298.15 K from the relation:[14]

$$\overline{V}_{m,i} = V_{m,i}^E + V_{m,i}^* + (1 - x_i)(dV_{m,i}^E / dx_i)_{T,P} \qquad (2)$$

where $V_{m,i}^*$ is the molar volume of the i^{th} component in the binaries. The derivatives $(\partial V_{m,i}^E / \partial x_i)_{T,P}$ were obtained by following a procedure (as detailed in chapter II) using the Redlich-Kister coefficients (a_i)[15] calculated for the excess molar volumes (V_m^E) for each binary mixture. The coefficients are: a_0 = 0.2216, a_1 = -0.8773, a_2 = -0.1140, a_3 = -0.1861 for the mixture (CH + MA); a_0 = -0.1250, a_1 = -0.9933, a_2 = -

0.1817, a_3 = 0.0495 for the mixture (CH + EA) and a_0 = -4.5071, a_1 = -0.9010, a_2 = -0.0375, a_3 = 0.5274 for the mixture (CH + MS) with standard deviations (σ) 0.045, 0.034, 0.054 for the corresponding mixtures, respectively. Partial molar volumes ($\overline{V}^{0}_{m,1}$ and $\overline{V}^{0}_{m,2}$) at infinite dilution, excess partial molar volumes ($\overline{V}^{E}_{m,i}$) and excess partial molar volumes ($\overline{V}^{0,E}_{m,i}$) at infinite dilution were determined at 298.15 K by using the standard relations described in chapter II.

Table 8.3. Molar volumes ($V^{*}_{m,1}$ and $V^{*}_{m,2}$), partial molar volumes at infinite dilution ($\overline{V}^{0}_{m,1}$ and $\overline{V}^{0}_{m,2}$) and excess partial molar volumes at infinite dilution ($\overline{V}^{0,E}_{m,1}$ and $\overline{V}^{0,E}_{m,2}$) for each component in the binary mixtures at 298.15 K; molar volumes are given in $cm^3 \cdot mol^{-1}$.

Parameters	CHN (1) +		
	MA (2)	EA (2)	MS (2)
$V^{*}_{m,1}$	104.23	104.23	104.23
$\overline{V}^{0}_{m,1}$	105.40	104.87	100.06
$V^{*}_{m,2}$	79.93	98.49	129.02
$\overline{V}^{0}_{m,2}$	78.97	97.24	124.10
$\overline{V}^{0,E}_{m,1}$	1.17	0.64	-4.17
$\overline{V}^{0,E}_{m,2}$	-0.96	-1.25	-4.92

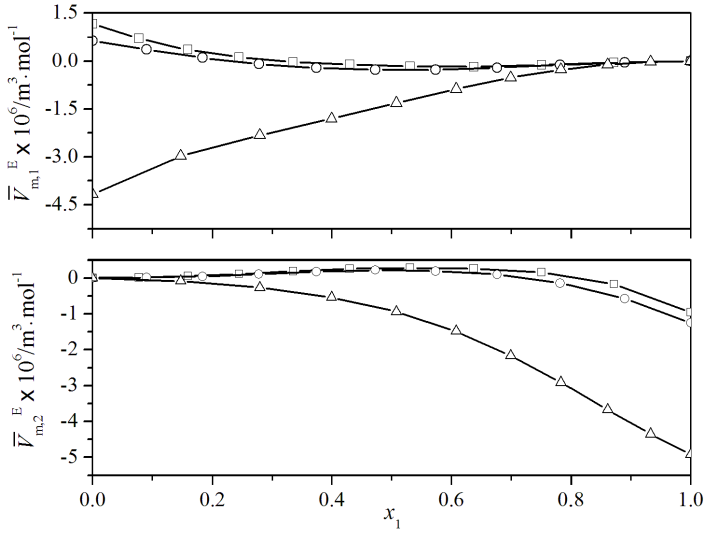

Fig. 8.2. Excess partial molar volume ($\overline{V}^{E}_{m,i}$) for the i^{th} component against mole fraction of CHN (x_1) for the binary mixtures of CHN with some esters at T = 298.15 K. The graphical points represent the $\overline{V}^{E}_{m,i}$ values for the mixtures with: □, MA; ○, EA; Δ, MS.

Molar volumes ($V^*_{m,1}$ and $V^*_{m,2}$), partial molar volumes ($\overline{V}^0_{m,1}$ and $\overline{V}^0_{m,2}$) and excess partial molar volumes ($\overline{V}^{0,E}_{m,i}$) at infinite dilution for each component in the mixtures at 298.15 K are listed in Table 8.3. Excess partial molar volumes ($\overline{V}^E_{m,1}$ and $\overline{V}^E_{m,2}$) of each component in the binary mixtures are depicted in Figure 8.2 against the mole fraction (x_1) of CHN. Figure 8.2 shows that $\overline{V}^E_{m,1}$ values gradually decrease (*i.e.*, decreasing trend as the alkyl chain length increases[9]) but $\overline{V}^E_{m,2}$ values increase with increasing mole fraction (x_1) of CHN for the mixtures studied. Partial molar volumes ($\overline{V}^0_{m,1}$) at infinite dilution for CHN in the mixtures (CHN + MA) and (CHN + EA) were found to be greater than its molar volume but those ($\overline{V}^E_{m,2}$) of the esters (MA and EA) were found to be lower than their respective molar volumes. These results corroborate with the interstitial accommodation of these ester molecules in the voids of CHN molecules and these ester molecules suffer volume contraction. Partial molar volumes ($\overline{V}^0_{m,1}$ and $\overline{V}^0_{m,2}$) at infinite dilution for both the components in the mixture (CHN + MS) were found to be lower than their respective molar volumes. These results, therefore, suggest the following order of packing efficiency or structure compactness in the mixtures: (CHN + MA) < (CHN + EA) < (CHN + MS).

8.3.2. Predictions of excess molar volumes

i) *Prigogine-Flory-Patterson theory* (PFP):

The Prigogine-Flory-Patterson (PFP) theory[5,6] can be used successfully to correlate, predict and estimate the excess molar volumes (V^E_m) of the binary mixtures theoretically. The interaction parameters ($\chi_{1,2}$) needed for the prediction of V^E_m values were obtained as described in chapter II and was adjusted by fitting the experimental V^E_m values over the entire composition at 298.15 K. According to this theory the excess molar volume (V^E_m) originates from a combination of interactional, a free volume and internal pressure contributions and V^E_m is given by:

$$\frac{V_m^E}{x_1V_1^* + x_2V_2^*} = \frac{(\tilde{v}^{1/3}-1)\tilde{v}^{2/3}\psi_1\theta_2}{[(4/3)\tilde{v}^{-1/3}-1]P_1^*}\chi_{1,2}$$

(interaction contribution)

$$-\frac{(\tilde{v}_1-\tilde{v}_2)^2[(14/9)\tilde{v}^{-1/3}-1]\psi_1\psi_2}{[(4/3)\tilde{v}^{-1/3}-1]\tilde{v}}$$

(free volume contribution)

$$+\frac{(\tilde{v}_1-\tilde{v}_2)(P_1^*-P_2^*)\psi_1\psi_2}{(P_1^*\psi_2+P_2^*\psi_1)}$$

(internal pressure contribution) (3)

where ψ_1 and ψ_2 stand for the molecular contact energy fractions of liquid 1 and liquid 2 in a mixture; θ_2 is the molecular site fraction of liquid 2 in a mixture and other symbols have their usual significance.[5,6] Various characteristic and reduced parameters of the pure liquid components such as reduced volume ($\tilde{v}$), reduced temperature ($\tilde{T}$), characteristic volume (V^*), characteristic pressure (P^*) and characteristic temperature (T^*) for each liquid component (needed for the V_m^E estimation) were calculated using Flory's formalism[16-19] and are listed in Table 8.4.

Table 8.4. Isobaric molar heat capacities (c_P), expansion coefficient (α), isothermal compressibility (κ_T) and Flory's parameters for pure liquids at 298.15 K.

Liquids	c_P [a]	$\tilde{v}$	$\tilde{T}$	$V^* \cdot 10^6$ ($m^3 \cdot mol^{-1}$)	P^* (Pa)	T^* (K)	α (kK^{-1})	κ_T (TPa^{-1})
CH	182.16	1.2407	0.0559	84.01	637.72	5333.17	0.9659	695.1
MA	141.93	1.3107	0.0658	60.98	609.89	4530.98	1.3250	1112.8
EA	170.66	1.3199	0.0670	74.62	605.88	4452.90	1.3756	1179.3
MS	249.06	1.2147	0.0517	106.22	692.34	5769.79	0.8433	535.8

[a]Values adapted from Ref. [13] were multiplied with molecular weight for unit conversion.

The interaction contributions to V_m^E were obtained from Eq. (3) by using a computer program as detailed in chapter II. The optimized $\chi_{1,2}$ values, calculated and experimental V_m^E values, their deviation and different contributions to V_m^E values at equimolar ($x_1 \approx 0.5$) composition at 298.15 K are given in Table 8.5. It reveals that the calculated excess molar volumes ($V_{m,PFP}^E$) reasonably agree with the experimental excess molar volumes (V_m^E) for all the mixtures studied.

Table 8.5. Interaction parameters ($\chi_{1,2}$), calculated and experimental values of excess molar volumes ($V^{E}_{m,exp}$ and $V^{E}_{m,PFP}$), their deviations (ΔV^{E}_{m}) and different contributions at 298.15 K.

CHN(1) +	$\chi_{1,2}$ ($J\cdot mol^{-1}$)	$V^{E}_{m,exp}\cdot 10^{6}$ ($m^3\cdot mol^{-1}$)	$V^{E}_{m,PFP}\cdot 10^{6}$ ($m^3\cdot mol^{-1}$)	$\Delta V^{E}_{m}\cdot 10^{6}$ ($m^3\cdot mol^{-1}$)	PFP contributions $\times 10^3$		
					int[a]	fv[b]	ip[c]
MA (2)	17.291	0.043	0.043	0.000	0.0031	0.0017	-0.0007
EA (2)	17.046	-0.005	-0.005	0.000	0.0033	0.0023	-0.0010
MS (2)	-78.873	-1.1289	-1.1289	0.000	-0.0111	0.0002	-0.0005

[a] interaction contribution; [b] free volume contribution; [c] internal pressure contribution

ii) *Peng-Robinson Equation of State* (PR-EOS):

Cubic equation of states are more commonly used in process simulations to correlate the solution properties and phase equilibria of hydrocarbon systems because they offer the best balance between accuracy, reliability, simplicity, computational efficiency and can also be extended to the liquid mixtures with different mixing or combination rules. Herein this chapter the classical cubic Peng-Robinson equation of state (PREOS) was used for correlating the excess molar volumes ($V^{E}_{m,\,PR\text{-}EOS}$) of the mixtures at 298.15 K. The two parametric PR-EOS is given by the relation:[8]

$$P = \frac{RT}{V-b} - \frac{a}{V(V+b)+b(V-b)} \qquad (4)$$

For a pure component the attraction parameter (a) and co-volume parameters (b) were obtained by using the standard relations as detailed in chapter II. However, acentric factor (ω) for each pure liquid was calculated from the relation:[20]

$$\omega = \frac{3T_{br}}{7(1-T_{br})}\log P_c - 1 \qquad (5)$$

where $T_{br} = T_b / T_c$ and T_b is the boiling point of a pure liquid. T_b, T_c and P_c values were taken from the literature.[13] For a binary mixture, the attraction parameter (a) and co-volume (b) parameters are given by the relations:[20]

$$a(T) = \sum_{i=1}^{2}\sum_{j=1}^{2} x_i x_j \sqrt{a_i a_j}(1-k_{ij}) \qquad (6)$$

$$b(T) = \sum_{i=1}^{2} x_i b_i \qquad (7)$$

where k_{ij} is the interaction coefficient for a binary mixture of components i and j and $k_{ij} = 0$ for i = j. On rearrangement in terms of the compressibility factor ($Z = PV/RT$), Eq. (4) becomes:

$$Z^3 - (1-B)Z^2 + (A - 3B^2 - 2B)Z - (AB - B^2 - B^3) = 0 \qquad (8)$$

where $B = Pb/RT$ and $A = aP/(RT)^2$. Thus from a knowledge of the compressibility factors of both the pure components and their mixtures the corresponding excess molar volumes ($V^E_{m,\,PR\text{-}EOS}$) of the binary mixtures were determined. The values of the interaction coefficient (k_{ij}) were found to be 0.0449, 0.0426 and -0.1672 with standard deviations (σ) 0.041, 0.055 and 0.069, respectively for the mixtures (CHN + MA), (CHN + EA) and (CHN + MS). A comparison between the experimental excess molar volumes (V^E_m) and the calculated excess molar volumes ($V^E_{m,\,PFP}$ and $V^E_{m,\,PR\text{-}EOS}$) as a function of mole fraction (x_1) of CHN for the studied mixtures at 298.15 K is depicted in Figure 8.3 and it is evident that the calculated excess molar volumes reasonably agree with the experimental excess molar volumes for all the studied mixtures.

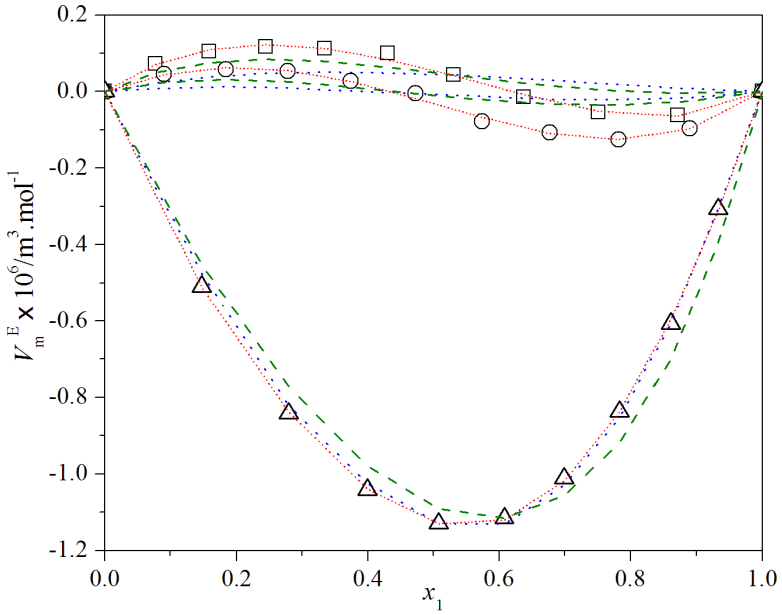

Fig. 8.3. A comparison between the excess molar volumes (V^E_m) *versus* mole fraction of CHN (x_1) for the binary mixtures of CHN (1) with some esters (2) at T = 298.15 K. The symbols represent experimental V^E_m values for the mixtures with: □, MA; ○, EA; Δ, MS. Olive dashed lines, PR-EOS; blue dotted lines, PFP; red short dotted lines, Redlich-Kister polynomial.

8.3.3. *Viscosity deviation*

The viscosity deviations ($\Delta\eta$) can be calculated by finding the difference between the measured viscosity (η) and the ideal viscosity (η_{id}) of a mixture as follows:

$$\Delta\eta = \eta - \eta_{id} \tag{9}$$

and the ideal viscosity (η_{id}) is given by:[21]

$$\eta_{id} = \exp(\sum_{i=1}^{2} x_i \ln\eta_{id}) \tag{10}$$

The uncertainty in viscosity deviation ($\Delta\eta$) was evaluated to be ±0.004 mPa s. Figure 8.4 ($\Delta\eta$ *versus* x_1 at 298.15 K) shows that the $\Delta\eta$ values are negative for the mixtures (CHN + MA) and (CHN + EA) but positive for the mixture (CH + MS) over the entire composition range. Similar composition dependence of $\Delta\eta$ values was observed at other experimental temperatures. The negative $\Delta\eta$ values suggest the easier flow of a liquid mixture in comparison to individual pure liquids. This is possibly due to the breaking of liquid order on mutual mixing and unfavorable nonspecific interactions amongst the unlike molecules. The positive $\Delta\eta$ values suggest the presence of strong intermolecular interactions amongst the unlike molecules leading to more compact structure.

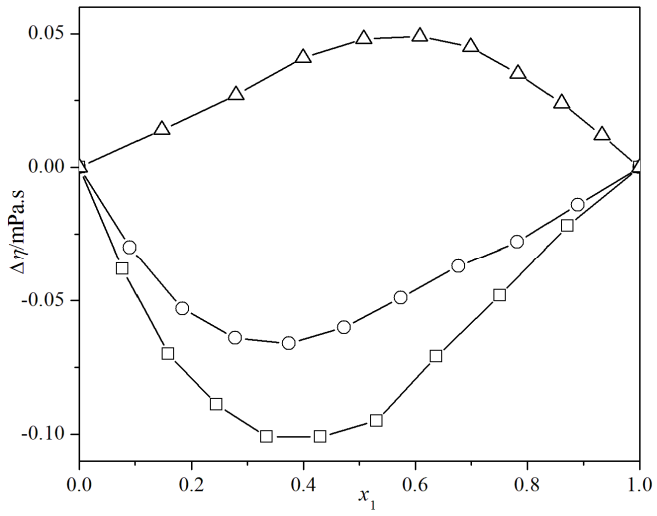

Fig. 8.4. Viscosity deviations ($\Delta\eta$) *versus* mole fraction of CHN (x_1) for the binary mixtures of CHN with some esters at T = 298.15 K. The symbols represent the $\Delta\eta$ values for the mixtures with: □, MA; ○, EA; Δ, MS.

Negative $\Delta\eta$ values for the mixtures (CHN + MA) and (CHN + EA) at dilute CHN range may be due to the molecular unpacking and unfavorable nonspecific interaction amongst the unlike components in the mixture. This effect is maximum at $x_1 \approx 0.3347$ and $x_1 \approx 0.3744$ for the mixtures (CHN + MA) and (CHN + EA), respectively at all the experimental temperatures. Beyond these compositions, however, the $\Delta\eta$ values increase due to increased dipole-dipole interactions and interstitial accommodation at CHN rich regions. On the contrary positive $\Delta\eta$ values for the mixture (CHN + MS) over the entire composition range suggest that the mixing of CHN with MS is characterized by strong intermolecular interactions amongst the component molecules due to dipole-dipole interactions, specific hydrogen bond interactions as well as interstitial accommodation. Thus the $\Delta\eta$ values also suggest the following order of molecular interactions in the mixtures: (CHN + MS) > (CHN + EA) > (CHN + MA). However, for each mixture the $\Delta\eta$ values decrease with a rise in the experimental temperatures and thus the molecular interactions amongst the dissimilar components become weaker at higher temperatures (Table 8.2.).

8.3.4. *Thermodynamics of viscous flow*

It is useful to study the activation parameters of viscous flow for a better understanding of different possible physico-chemical interactions prevailing in the mixtures and such parameters can be evaluated using viscosities of the mixtures in terms of Eyring's theory of absolute reaction rate[21] as expressed by the relation:

$$\eta = \left(\frac{hN}{V}\right)\exp\left(\frac{\Delta G^*}{RT}\right) \qquad (11)$$

Substituting $\Delta G^* = \Delta H^* - T\Delta S^*$ in Eq. (11), we get:

$$R\ln\left(\frac{\eta V}{hN}\right) = \frac{\Delta H^*}{T} - \Delta S^* \qquad (12)$$

where N is Avogadro's number, h is Planck's constant, ΔG^*, ΔH^* and ΔS^* are the activation free energy, enthalpy and entropy for viscous flow and other symbols have their usual meanings. Therefore linear regressions of $R\ln(\eta V/hN)$ against $(1/T)$ yield the enthalpy (ΔH^*) and entropy (ΔS^*) of activation of viscous flow from the corresponding slope and intercept, respectively.

Again the excess free energy of activation of viscous flow of the mixtures (ΔG^{*E}) can be had from the relation:

$$\Delta G^{*E} = \Delta G^{*} - \sum_{i=1}^{2} (x_i \Delta G_i^{*E}) \qquad (13)$$

ΔG^{*}, ΔH^{*}, ΔS^{*} and the regression coefficients (R^2) are given in Table 8.6. Table 8.6 manifests that ΔH^{*} values are positive for all the mixtures but ΔS^{*} values are mostly negative for the mixtures (CHN + EA) and (CHN + MS) except the mixture (CHN + MA). Interestingly ΔS^{*} values decrease or become more negative in the order: (CHN + MA) > (CHN + EA) > (CHN + MS) in parallel to the extent of molecular compactness as discussed above. Excess free energies of activation of viscous flow (ΔG^{*E}) were plotted in Figure 8.5 against the mole fraction (x_1) of CHN for all the mixtures at 298.15 K. According to Reid and Taylor[22] positive ΔG^{*E} may be ascribed to molecular interactions or structural compactness due to geometrical fittings of one component into the other's structure in the mixture and negative ΔG^{*E} values may be ascribed to the dominance of dispersion forces allowing easier fluid flow.

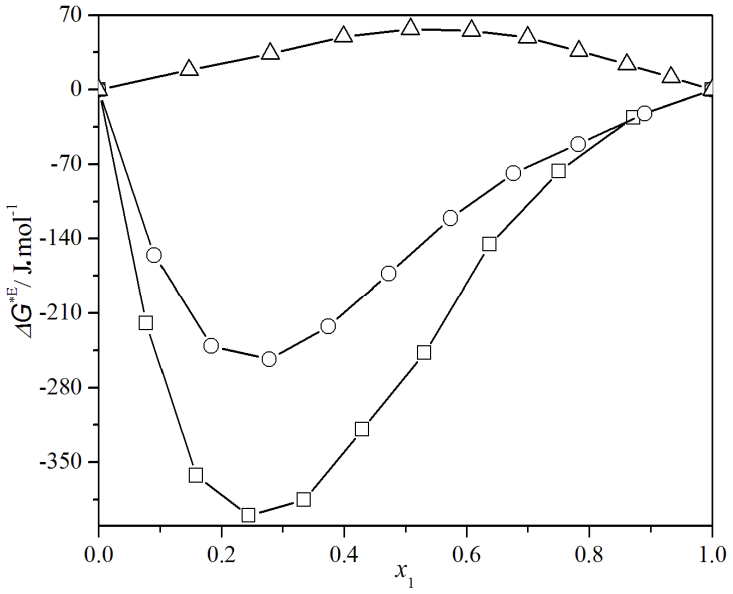

Fig. 8.5. Excess free energy of activation of viscous flow (ΔG^{*E}) *versus* mole fraction of CH (x_1) for the binary mixtures of CHN with some esters at T = 298.15 K. The symbols represent the ΔG^{*E} values for the mixtures with: □, MA; ○, EA; Δ, MS.

Table 8.6. Free energy (ΔG^*), enthalpy (ΔH^*) and entropy (ΔS^*) of activation of viscous flow for the binary mixtures; x_1-mole fraction of CHN.

x_1	ΔG^* ($kJ \cdot mol^{-1}$)			ΔH^* ($kJ \cdot mol^{-1}$)	ΔS^* ($J \cdot K^{-1} \cdot mol^{-1}$)	R^2
	298.15 K	308.15 K	318.15 K			
			CHN (1) + MA (2)			
0	10.744	10.914	11.019	6.647	-13.777	0.9927
0.0774	10.896	10.929	10.671	14.193	10.907	0.9677
0.1587	11.143	11.006	10.601	19.174	26.797	0.9848
0.2444	11.516	11.227	10.794	22.253	35.938	0.9967
0.3347	11.964	11.618	11.231	22.890	36.624	0.9997
0.4301	12.487	12.250	11.923	20.881	28.104	0.9986
0.5310	13.043	12.905	12.696	18.195	17.243	0.9988
0.6378	13.657	13.570	13.425	17.099	11.515	0.9991
0.7512	14.269	14.254	14.193	15.405	3.784	0.9993
0.8717	14.898	14.932	14.938	14.287	-2.063	0.9997
1	15.539	15.579	15.625	14.254	-4.308	0.9999
			CHN (1) + EA (2)			
0	11.541	11.718	11.915	5.956	-18.721	0.9991
0.0907	11.748	11.796	11.845	10.303	-4.844	0.9999
0.1833	12.032	12.053	12.026	12.113	0.246	0.9988
0.2778	12.398	12.398	12.377	12.709	1.033	0.9998
0.3744	12.815	12.819	12.829	12.609	-0.688	0.9999
0.4730	13.259	13.279	13.300	12.647	-2.052	0.9999
0.5738	13.714	13.746	13.765	12.960	-2.536	0.9999
0.6768	14.169	14.206	14.244	13.037	-3.794	0.9999
0.7822	14.617	14.670	14.726	12.995	-5.439	0.9999
0.8899	15.076	15.117	15.162	13.791	-4.307	0.9999
1	15.539	15.579	15.625	14.254	-4.308	0.9999
			CHN (1) + MS (2)			
0	15.387	15.693	16.029	5.825	-32.055	0.9977
0.1469	15.428	15.695	15.986	7.116	-27.869	0.9991
0.2793	15.464	15.696	15.949	8.232	-24.245	0.9995
0.3992	15.498	15.694	15.912	9.333	-20.665	0.9996
0.5082	15.521	15.687	15.873	10.289	-17.538	0.9997
0.6079	15.535	15.672	15.831	11.134	-14.750	0.9997
0.6993	15.543	15.655	15.787	11.905	-12.189	0.9998
0.7834	15.543	15.635	15.744	12.538	-10.068	0.9998
0.8611	15.542	15.614	15.701	13.164	-7.966	0.9999
0.9331	15.541	15.596	15.660	13.764	-5.955	0.9999
1	15.539	15.579	15.625	14.254	-4.308	0.9999

Therefore the observed negative ΔG^{*E} values (Figure 8.5) suggest the easier viscous flow for the mixtures (CHN + MA) and (CHN + EA) as compared to the mixture (CHN + MS). Similar composition dependence of ΔG^{*E} values was observed at other experimental temperatures.

8.3.5. *Viscosity correlation*

Several empirical and semi-empirical relations are used to represent the composition dependence of viscosity in binary liquid mixtures as well as to simulate the viscosity of liquids or liquid mixtures.[23] Such empirical methods have also been developed using the corresponding state principle based on van der Waals' hypothesis.[24] Herein this chapter the experimental viscosities at 298.15 K were correlated with models like Bloomfield-Dewan,[7] cubic equation of state based Peng-Robinson,[8] Grunberg-Nissan,[25] and Katti-Choudhury.[26]

i) *Peng-Robinson Equation of State* (PR-EOS):

In this viscosity model Eyring's viscosity expression for liquid mixtures is coupled with Peng-Robinson equation of state. The final form of the viscosity expression is given by:[27]

$$\eta = \frac{(\eta V)^{id}}{V_m} \exp\left[\sum_{i=1}^{2} x_i (\ln \varphi_i - \ln \varphi_i^0) + \frac{1}{2}\sum_{i=1}^{2}\sum_{j=1}^{2} x_i x_j g_{ij}\right] \qquad (14)$$

where V_m, $(\eta V)^{id}$, φ_i^0, φ_i and g_{12} ($g_{ii} = 0$ and $g_{ij} = g_{ji}$) are the molar volume, kinematic viscosity of an ideal mixture, fugacity coefficients of the i^{th} component in pure state, fugacity coefficients of the i^{th} component in a mixture and binary interaction parameter, respectively. The details of the model have been described in chapter II. In order to obtain the binary interaction parameter (g_{12}), a non-linear regression analysis was performed to have minimum standard deviation (σ) for a binary mixture. The binary interaction parameters (g_{12}) were found to be –0.571 (σ = 0.055), -0.505 (σ = 0.033) and –0.131 (σ = 0.002) for the mixtures (CHN + MA), (CHN + EA) and (CHN + MS), respectively.

ii) *Bloomfield-Dewan viscosity model*:

Bloomfield and Dewan developed this model by combining the absolute reaction rate theory[21] and the free volume theory,[28] which treats the properties of a mixture in terms of reduced properties of the pure components. The expression proposed for the viscosity deviation ($\Delta \ln \eta$) of a mixture is given by:

$$\Delta \ln \eta = f(\tilde{v}) - \frac{\Delta G^R}{RT} \qquad (15)$$

$$\Delta \ln \eta = \ln \eta - \sum_{i=1}^{2} (x_i \eta_i) \qquad (16)$$

where $f(\tilde{v})$ and ΔG^{R} are the characteristic function of the free volume and the residual free energy of mixing, respectively. These quantities were obtained by using the standard literature relations.[28] Based on Flory's statistical thermodynamic theory for liquid mixtures,[16-19] the excess energy ΔG^{E} can be obtained from the relation:

$$\Delta G^{E} = \sum_{i=1}^{2} x_i P_i^* V_i^* [(1/\tilde{v}_i - 1/\tilde{v}) + 3\tilde{T}_i \ln\{(\tilde{v}_i^{1/3} - 1)/(\tilde{v}^{1/3} - 1)\}] + (x_1 \theta_2 V_1^* \chi_{12})/\tilde{v} \quad (17)$$

The standard deviations (σ) between the experimental viscosities and those calculated from Bloomfield and Dewan model were 0.115, 0.207 and 0.189 for the mixtures of (CHN + MA), (CHN + EA) and (CHN + MS), respectively. Experimental viscosities were also correlated with Grunberg-Nissan (GN) and Katti-Chaudhri (KC) viscosity models at 298.15 K using required regressions. While Grunberg-Nissan parameters (d_{12}) were determined to be -0.546 (σ = 0.058), -0.307 (σ = 0.350) and 0.102 (σ = 0.003); Katti-Chaudhri parameter (W_{vis}/RT) were found to be -105.52 (σ = 0.057), -63.65 (σ = 0.034) and 17.76 (σ = 0.002), respectively for the mixtures (CHN + MA), (CHN + EA) and (CHN + MS). The variations of experimental and theoretical viscosities with the mole fraction (x_1) of CHN at 298.15 K are depicted in Figure 8.6.

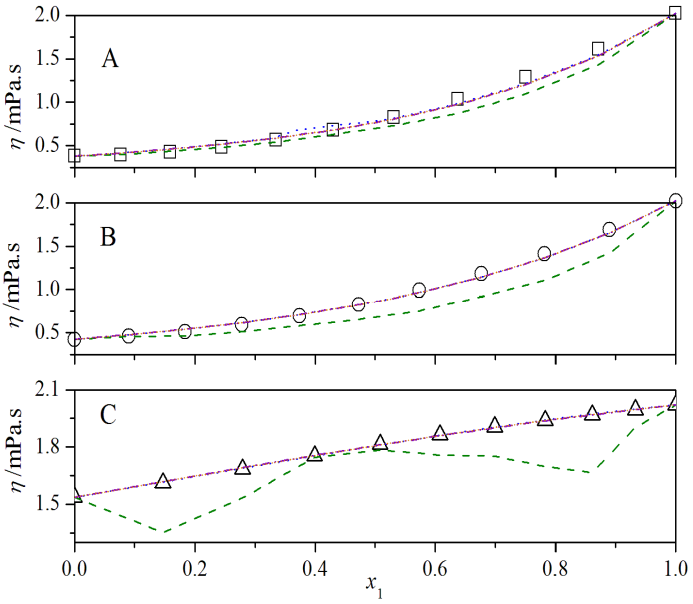

Fig. 8.6. A comparison between the viscosities (η) *versus* mole fraction of CHN (x_1) for the binary mixtures at T = 298.15 K: A, CHN (1) + MA (2); B, CHN (1) + EA (2); C, CHN (1) + MS (1). The symbols represent experimental η values for the mixtures with: □, MA; ○, EA; Δ, MS. Olive dashed lines, BF; blue dotted lines, PREOS; violet dash dotted lines, GN; orange short dotted lines, KC.

8.3.6. *Ultrasonic speed of sound and derived functions*

The ultrasonic speed of a liquid is fundamentally related to binding forces amongst component molecules and has been successfully employed to provide qualitative information regarding the physical nature and strength of molecular interactions in pure liquid as well as in liquid mixtures. The experimental speeds of sound (u) and the densities (ρ) of the binary mixtures at 298.15 K were used to determine the isentropic compressibilities (κ_S) and other acoustic parameters along with the corresponding excess or deviation functions. The excess isentropic compressibilities (κ_S^E) were obtained from the relation:

$$\kappa_S^E = \kappa_S - \kappa_S^{id} \tag{18}$$

where κ_s is the isentropic compressibility and was calculated using the Laplace relation, $\kappa_s = 1/\rho u^2$ and κ_s^{id} is the isentropic compressibility for an ideal mixture. According to Benson and Kiyohara[29] and Acree,[30] κ_s^{id} is given by the relation:

$$\kappa_S^{id} = \sum_{i=1}^{2} \tau_i \left[\kappa_{S,i} + \frac{T V_{m,i}^{*} \alpha_i^{2}}{c_{P,i}} \right] - \left\{ \frac{T \sum_{i=1}^{2} (x_i V_{m,i}^{*}) \sum_{i=1}^{2} (\tau_i \alpha_i)^2}{\sum_{i=1}^{2} (x_i c_{P.i})} \right\} \tag{19}$$

where τ_i is the volume fraction of the i^{th} component in the mixture, $\kappa_{s,i}$, $V_{m,i}^{*}$, α_i and $c_{p,i}$ are the isentropic compressibility, molar volume, isobaric expansion coefficient and molar isobaric heat capacity of the pure components, respectively. Isobaric expansion coefficients (α_i) were obtained from experimental densities and $c_{p,i}$ values were adapted from the literature.[13] The other acoustic parameters like intermolecular free lengths (L_f) and free volumes (V_f) and their excess values were calculated as described in chapter II. The parameters u, κ_s and κ_S^E at 298.15 K are listed in Table 8.7. The experimental speeds of sound of each pure liquid were in good agreement with the literature values[31-34] at 298.15 K. Figure 8.7 represents the variation of excess isentropic compressibilities (κ_S^E) of the mixtures against the mole fraction (x_1) of CHN at 298.15 K. While excess isentropic compressibilities (κ_S^E) for the mixture (CHN + MA) were mostly positive, those for the mixtures (CHN + EA) and (CHN + MS) were mostly negative. Positive κ_S^E values for the mixture (CHN + MA) suggest perturbation of the associated structures or molecular order in the pure liquids leading

Table. 8.7. Ultrasonic speeds (u), isentropic compressibilities (κ_S), intermolecular free lengths (L_f), free volumes (V_f), excess isentropic compressibilities (κ_S^E), excess intermolecular free lengths (L_f^E) and excess free volumes (V_f^E) for the binary mixtures at 298.15 K; x_1-mole fraction of CHN.

x_1	u / m · s^{-1}	κ_S / TPa^{-1}	L_f /Å	$V_f \cdot 10^8$ / m^3 · mol^{-1}	κ_S^E / TPa^{-1}	L_f^E /Å	$V_f^E \cdot 10^8$ / m^3 · mol^{-1}
CHN (1) + MA (2)							
0	1148.5	818.0	0.5883	37.70	0	0	0
0.0774	1148.8	817.0	0.5879	37.04	25.1	0.0083	1.76
0.1587	1155.3	806.8	0.5842	34.65	41.4	0.0138	1.92
0.2444	1170.9	784.3	0.5760	30.44	45.9	0.0152	0.39
0.3347	1193.0	754.3	0.5649	25.81	43.3	0.0142	-1.40
0.4301	1223.3	716.1	0.5504	21.15	33.1	0.0104	-3.77
0.5310	1256.8	676.9	0.5351	17.08	22.4	0.0064	-3.99
0.6378	1295.9	635.3	0.5184	13.42	9.6	0.0017	-4.31
0.7512	1334.5	597.9	0.5029	10.56	1.6	-0.0011	-3.61
0.8717	1371.3	565.3	0.4890	8.23	-1.0	-0.0015	-2.17
1	1407.7	535.9	0.4761	6.38	0	0	0
CHN (1) + EA (2)							
0	1144.3	853.7	0.6010	41.09	0	0	0
0.0907	1160.7	826.0	0.5911	37.93	0.3	0.0015	-0.01
0.1833	1177.9	798.1	0.5811	33.43	0.7	0.0030	-1.30
0.2778	1197.4	768.4	0.5701	28.13	0.4	0.0039	-3.32
0.3744	1220.1	736.1	0.5580	23.02	-1.5	0.0038	-5.08
0.4730	1247.3	700.5	0.5444	18.63	-5.9	0.0025	-6.05
0.5738	1277.8	663.6	0.5298	15.02	-10.7	0.0005	-6.16
0.6768	1311.3	626.7	0.5149	12.16	-14.5	-0.0016	-5.44
0.7822	1346.5	591.2	0.5001	9.89	-15.9	-0.0032	-4.05
0.8899	1379.6	560.4	0.4869	7.97	-11.6	-0.0030	-2.23
1	1407.7	535.9	0.4761	6.38	0	0	0
CHN (1) + MS (2)							
0	1410.9	426.0	0.4245	18.66	0	0	0
0.1469	1421.1	428.7	0.4259	16.17	-11.4	-0.0062	-0.69
0.2793	1427.5	434.1	0.4285	14.13	-19.4	-0.0104	-1.10
0.3992	1430.8	441.7	0.4323	12.41	-24.3	-0.0129	-1.35
0.5082	1430.4	451.8	0.4372	11.01	-26.0	-0.0135	-1.41
0.6079	1424.3	466.1	0.4441	9.83	-22.8	-0.0118	-1.37
0.6993	1419.5	480.2	0.4507	8.88	-19.2	-0.0099	-1.20
0.7834	1413.9	495.3	0.4577	8.09	-14.0	-0.0072	-0.95
0.8611	1412	508.3	0.4637	7.44	-10.4	-0.0053	-0.64
0.9331	1409.7	522.1	0.4700	6.88	-5.4	-0.0027	-0.32
1	1407.7	535.9	0.4761	6.38	0	0	0

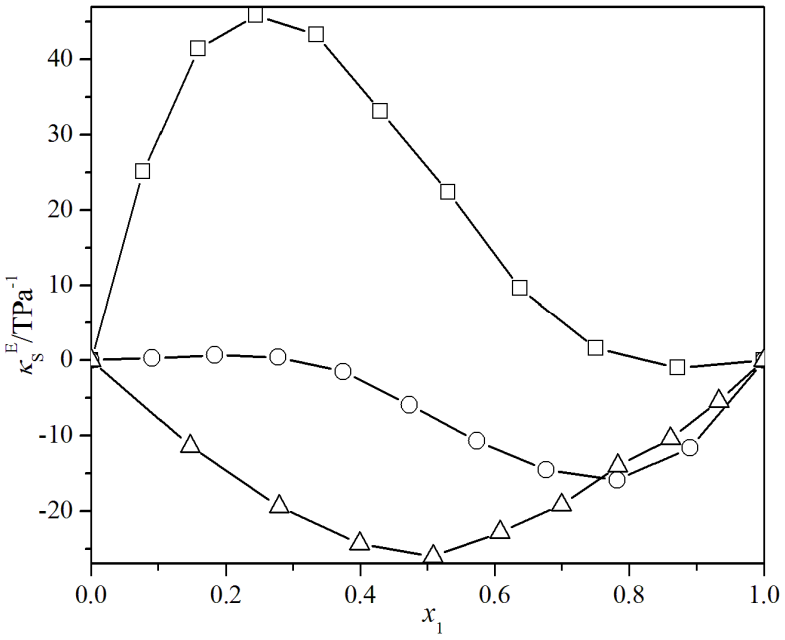

Fig. 8.7. Excess isentropic compressibility (κ_S^E) *versus* mole fraction of CHN (x_1) for the binary mixtures of CH + some esters at T = 298.15 K. The graphical points represent the κ_S^E values for the mixtures with: □, MA; ○, EA; Δ, MS.

to breaking up of the weak dipole-dipole cohesive forces operating amongst the similar molecules on mutual mixing. Negative κ_S^E values for the mixtures (CHN + EA) and (CHN + MS) are associated with structure making or more compact packing of the dissimilar molecules due to combined effects of specific hydrogen bond interactions, dipole-dipole interactions and interstitial accommodation. It is interesting that the speeds of sound (u) increase as the molecular compactness increase for the mixtures. Furthermore, the intermolecular free length, *i.e.*, the distance between the surfaces of neighboring molecules, is generally found to show an opposite behavior to those of ultrasonic speeds, *i.e.*, the decrease in intermolecular free length increases the ultrasonic speeds and acoustic impedances. The decrease in intermolecular free length and increase in ultrasonic speeds and acoustic impedances signify the molecular interactions amongst the component molecules in the mixtures. Variations of these acoustic parameters and the corresponding excess functions with mole fractions (x_1) of CHN at 298.15 K are in Table 8.7. The perusal of Table 8.7 shows that the excess free lengths (L_f^E) are positive in the ester rich region and negative in CHN rich region

for the mixtures (CHN + MA) and (CHN + EA) but are negative for the mixture (CHN + MS) throughout the entire composition range at 298.15 K. Interestingly, it was observed that free volumes (V_f) and excess free volumes (V_f^E) for the mixtures studied followed the order: (CHN + MA) > (CHN + EA) > (CHN + MS), *i.e.*, the reversed order of molecular interactions in parallel to the degree of their structural compactness. Thus the study of the various acoustic and their excess functions also stand in support of the order of molecular interactions discussed on the basis of excess molar volumes and viscosity deviations.

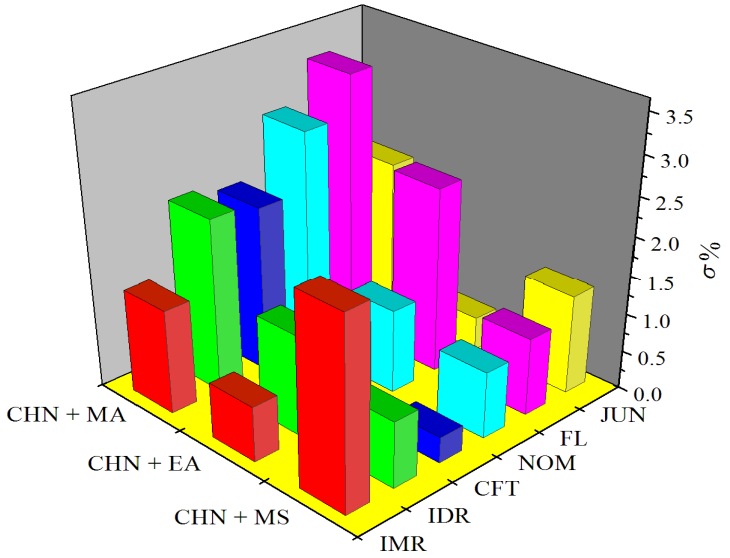

Fig. 8.8. Percent standard deviations ($\sigma\%$) for theoretical prediction of ultrasonic speeds by different empirical relations at T = 298.15 K for the binary mixtures studied.

8.3.7. *Prediction of ultrasonic speed of sound*

The experimentally determined ultrasonic speeds (u) of sound for the studied mixtures were compared with the ultrasonic speeds obtained from Flory theory (FL), Collision factor theory (CFT), Nomoto relation (NOM), Impedance dependence relation (IDR), Ideal mixture relation (IMR) and Junjie's relation (JUN). These empirical models are well described in chapter II. A comparison of the percent standard deviations ($\sigma\%$) reveals that predictive capabilities of these models follow the order: FL > IMR > JUN > CFT > IDR > NOM (for CHN + MA mixture); JUN > IMR > NOM > CFT > IDR > FL (for CHN + EA mixture) and CFT > NOM ≈ IDR > JUN > IMR > FL (for CHN + MS mixture), respectively (Figure 8.8.).

8.3.8. *Excess molar refractions*

The study of refractive indices (n_D), molar refractions (R_m) and the excess molar refractions (R_m^E) plays an important role in explaining the molecular interactions in the binary mixtures. The excess molar refractions (R_m^E) for the mixtures were obtained from relation:[35]

$$R_m^E = R_m - \sum_{i=1}^{2}(x_i R_{m,i}) \qquad (20)$$

where $R_{m,i} = \{(n_{D,i}-1)/(n_{D,i}+2)\}M_i/\rho_i$, $n_{D,i}$ and ρ_i stand for the molar refraction, refractive index and density of the ith component in the mixture, respectively. The molar refractions (R_m) for a mixture can be had from the relation:[35]

$$R_m = \frac{n_D^2 - 1}{n_D^2 + 2}\frac{\sum_{i=1}^{2} x_i M_i}{\rho} \qquad (21)$$

where ρ and n_D are the mixture density and refractive index; M_i stands for the molar mass of ith component in a mixture, respectively. Molar refractions (R_m), excess molar refractions (R_m^E) and the experimental refractive indices (n_D) for the three binaries are listed in Table 8.8. The experimental refractive indices (n_D) of the pure liquids were in good agreement with literature values[12,31,36] at 298.15 K and the trends in excess molar refractions (R_m^E) for the binary mixtures with respect to composition were found to be in line with the molecular interactions discussed above.

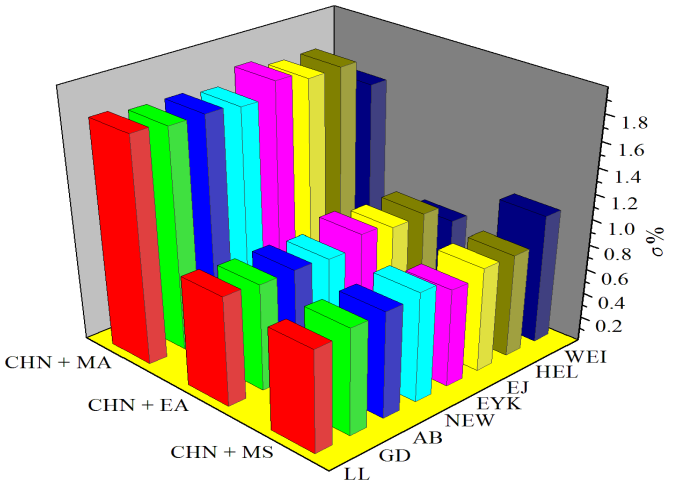

Fig. 8.9. Percent standard deviations ($\sigma\%$) for theoretical prediction of refractive indices by various models at T = 298.15 K for the binary mixtures studied.

Table 8.8. Refractive indices (n_D), molar refractions (R_m) and excess molar refractions (R_m^E) for the binary mixtures at 298.15 K; x_1-mole fraction of CHN.

x_1	n_D	$R_m \cdot 10^6$ $(m^3 \cdot mol^{-1})$	$R_m^E \cdot 10^6$ $(m^3 \cdot mol^{-1})$
CHN (1) + MA (2)			
0	1.3604	17.658	0
0.0774	1.3808	19.003	0.550
0.1587	1.4001	20.342	1.054
0.2444	1.4181	21.674	1.506
0.3347	1.4328	22.908	1.813
0.4301	1.4428	23.978	1.904
0.5310	1.4489	24.907	1.797
0.6378	1.4506	25.671	1.465
0.7512	1.4486	26.300	0.930
0.8717	1.4476	27.031	0.424
1	1.4484	27.9249	0
CHN (1) + EA (2)			
0	1.3712	22.343	0
0.0907	1.3861	23.274	0.425
0.1833	1.3978	24.029	0.663
0.2778	1.4079	24.699	0.806
0.3744	1.4170	25.316	0.884
0.4730	1.4256	25.910	0.926
0.5738	1.4331	26.439	0.893
0.6768	1.4398	26.943	0.822
0.7822	1.4446	27.354	0.645
0.8899	1.4468	27.644	0.334
1	1.4484	27.925	0
CHN (1) + MS (2)			
0	1.5352	40.179	0
0.1469	1.5199	37.954	-0.425
0.2793	1.5062	36.036	-0.720
0.3992	1.4914	34.222	-1.065
0.5082	1.4785	32.664	-1.287
0.6079	1.4682	31.378	-1.352
0.6993	1.4595	30.284	-1.326
0.7834	1.4542	29.465	-1.114
0.8611	1.4506	28.806	-0.820
0.9331	1.4503	28.390	-0.354
1	1.4484	27.925	0

Refractive indices were also predicted by models like Lorentz-Lorenz (LL), Gladstone-Dale (GD), Arago-Biot (AB), Newton (NEW), Eykman (EYK), Eyring-John (EJ), Heller (HEL), and Weiner (WEI) as detailed in chapter II and references therein.[37,38] The correlating abilities of these models were ascertained by percent standard deviations ($\sigma\%$) and a comparison has been illustrated in Figure 8.9.

8.3.9. *IR spectroscopic study*

The results obtained so far are also well reflected in FT-IR spectra of the binary mixtures (Figures 8.10-8.12). The spectra were recorded in a demountable KBr cell for liquid samples with spacer of path length of 0.5 mm at ambient temperature with a Perkin-Elmer Spectrum FT-IR spectrometer (RX-1). MA and EA show characteristic C=O stretching vibrations at 1760 and 1739 cm^{-1}, respectively along with some C-H stretching vibrations in the range 3000-2800 cm^{-1}. In the structure of CHN, chair type monomers were reported to form $C-H\cdots O-$ bonded dimmers through the involvement of –C=O group[39] and the corresponding band appearing at around 1713 cm^{-1} is thus broad and strong enough. Gradual intensity loss and shifting to higher frequencies of this band with the advent of the esters (MA and EA) suggests breaking of intermolecular $C-H\cdots O$ interactions within CHN molecules and formation of intermolecular $C-H\cdots O$ interactions between CHN and the ester molecules.

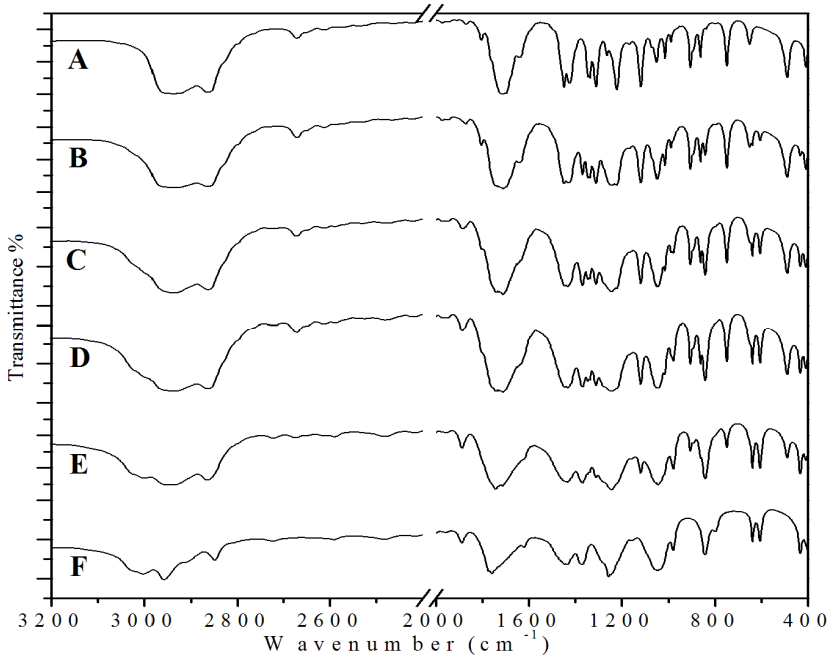

Fig. 8.10. FTIR spectra of the various binary mixtures of CHN (1) + MA (2): A, pure CHN (x_2 = 0.00); B, x_2 = 0.20; C, x_2 = 0.40; D, x_2 = 0.60; E, x_2 = 0.80; F, pure MA (x_2 = 1.00).

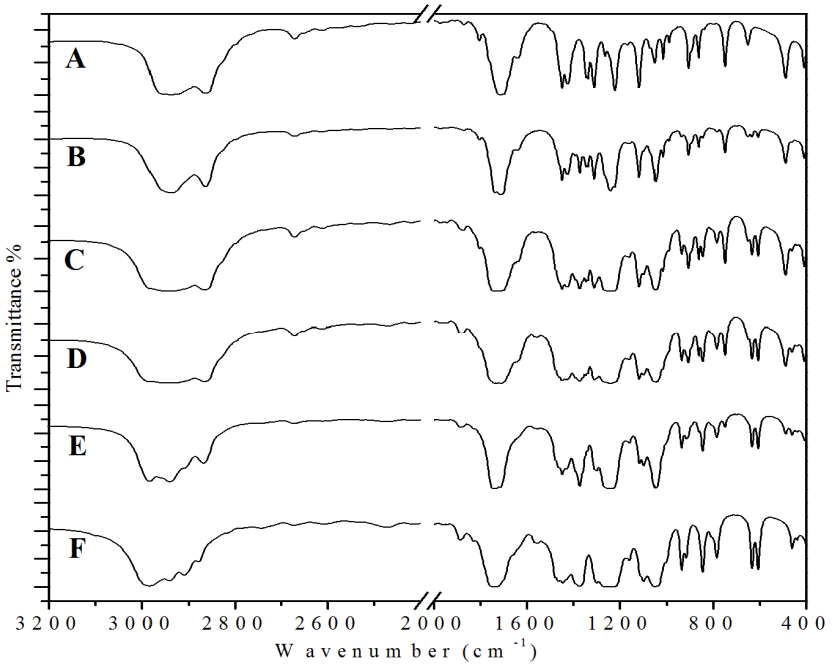

Fig. 8.11. FTIR spectra of the various binary mixtures of CHN (1) + EA (2): A, pure CHN (x_2 = 0.00); B, x_2 = 0.20; C, x_2 = 0.40; D, x_2 = 0.60; E, x_2 = 0.80; F, pure EA (x_2 = 1.00).

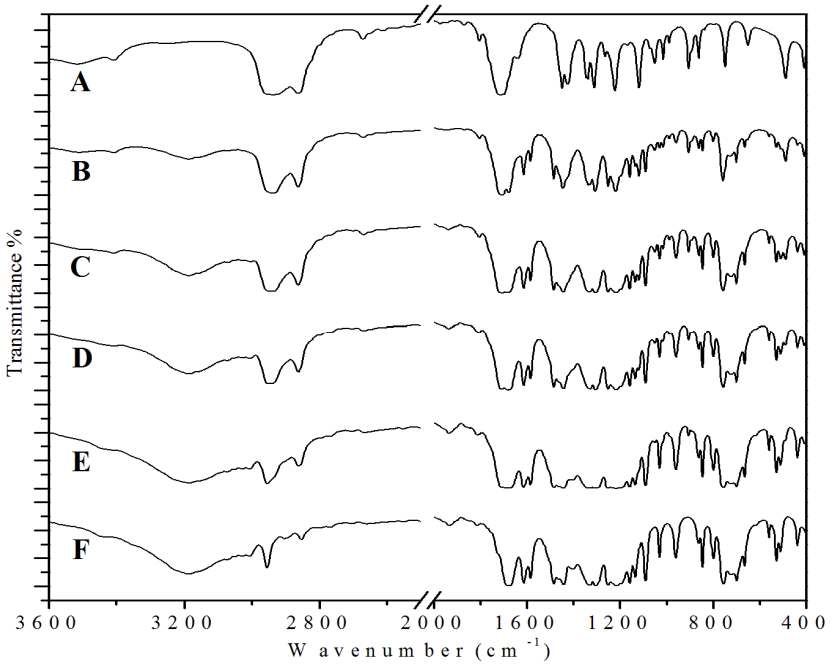

Fig. 8.12. FTIR spectra of the various binary mixtures of CHN (1) + MS (2): A, pure CHN (x_2 = 0.00); B, x_2 = 0.20; C, x_2 = 0.40; D, x_2 = 0.60; E, x_2 = 0.80; F, pure MS (x_2 = 1.00).

Again the band near 2960 cm^{-1} due to C-H stretching vibrations of CHN losses intensity on dilution with the esters (MA and EA) and thus behaves like the hydrogen bonded carbonyl band $\nu_{C=O(\cdots H)}$ and shows a blue shifted $\nu_{C\text{-}H(\cdots O)}$ mode.[39] MS shows characteristic bands around 3180 cm^{-1} and 1676 cm^{-1} due to hydrogen bonded –OH and –C=O groups, respectively. The –C=O stretching band becomes broader as the mole fraction (x_1) of CHN increases in this mixture and splits into a doublet at x_1 = 0.80.[40] Again the broad band at 3180 cm^{-1} losses intensity on dilution with CHN; in consequence the bands appearing in the range 3000-2800 cm^{-1} due to C-H stretching vibrations appear more intense. These facts corroborate with the presence of strong intermolecular hydrogen bond interactions in the mixture (CHN + MS). However, the weak bands appearing in the region 3600-3400 cm^{-1} for MA, EA and CHN probably originates from some overtone or other combination bands and as such they were kept out of present analysis.

8.4. Conclusion

In summary, the various derived properties reveal the following order of molecular interactions: (CHN + MS) > (CHN + EA) > (CHN + MA) for the mixtures studied. Such an order of molecular interactions originates from a combined effect of factors like the molecular size, shape and nature of the components. This order can be attributed to the breaking up of dipolar interactions or the three-dimensional hydrogen bonded network (through inter- or intra-molecular), interstitial accommodation as well as intermolecular hydrogen bond interactions on mutual mixing of the components. A comparison of the excess partial molar volumes ($\overline{V}^{0,E}_{m,1}$ and $\overline{V}^{0,E}_{m,2}$) at infinite dilution to the molar volumes of the pure components in the studied mixtures suggests that the molecular compactness increases in the same ascending order of molecular interactions shown above. FT-IR spectra of the mixtures also correlate well with the observed molecular interactions for the mixtures studied.

References

[1] C.R. Reid, B.E. Poling, *The properties of Gases and Liquids*, McGraw Hill, New York, 1998, Ch.1.

[2] J.G. Harris, F.H. Stillinger, J. Chem. Phys.**,** 95 (1991) 5953.

[3] F. Nabi, M.A. Malik, C.G. Jesudason, S.A.Al-Thabaiti, Korean. J. Chem. Eng., 31 (2014) 1505.

[4] G.A. Krestov, *Thermodynamics of Solvation; Solution and Dissolution, Ions and Solvents, Structure and Energetics*, Ellis Horwood, New York, 1991, pp. 151.

[5] D. Patterson, G. Delmas, J. Polym. Sci., 30 (1970) 1.

[6] D. Patterson, Pure. Appl. Chem., 47 (1976) 305.

[7] V.A. Bloomfield, R.K. Dewan, J. Phys. Chem., 75 (1971) 3113.

[8] D.Y. Peng, D.B. Robinson, Ind. Eng. Chem. Fundum., 15 (1976) 59.

[9] M.N. Roy, B.K. Sarkar, B. Sinha, J. Chem. Eng. Data 54 (2009) 1076.

[10] J.A. Riddick, W.B. Bunger, T.K. Sakano, *Organic Solvents: Physical Properties and Methods of Purification*, 4th ed., Wiley: New York, 1986.

[11] R. Venis, R. Rajkumar, J. Chem. Pharm. Res., 2 (2011) 878.

[12] T.M. Aminabhavi, H.T.S. Phayde, J. Chem. Eng. Data 41(1996) 813.

[13] W.M. Haynes, D.R. Lide, T.J. Bruno, *CRC Handbook of Chemistry & Physics*, 93rd edn., Taylor & Fransis¸ Boca Roton, London, 2012-2013.

[14] G.M. Smith, H.C. Van Ness, *Introduction to Chemical Engineering Thermodynamics*, McGraw Hill, New York, 1987.

[15] O. Redlich, A.T. Kister, Indus. Eng. Chem., 40 (1948) 345.

[16] P.J. Flory, R.A. Orwell, A. Vriji, J. Am. Chem. Soc., 86 (1964) 3507.

[17] P.J. Flory, R.A. Orwell, A. Vriji, J. Am. Chem. Soc., 86 (1964) 3515.

[18] P.J. Flory, J. Am. Chem. Soc., 87 (1965) 1833.

[19] A. Abe, P.J. Flory, J. Am. Chem. Soc., 87 (1965) 1838.

[20] S.I Sandler, *Chemical, Biochemical, and Engineering Thermodynamics*, 4th edn., John Wiley & Sons (Asia), New Delhi, 2006, pp. 242, 258.

[21] S. Glasstone, K.J. Laidler, H. Eyring, *The theory of Rate Preocess*, McGraw-Hill Book Comnpany, New York, 1941.

[22] T.M. Reid, T.E. Taylor, J. Phys. Chem., 63 (1949) 58.

[23] A.K. Mehrotra, W.D. Monnery, W. Svrcek, Fluid Phase Equilib., 117 (1996) 344.

[24] R.D. McCarty, Fluid Phase Equilib., 256 (2007) 42.

[25] L. Grunberg, A.H. Nissan, Nature, 164 (1949) 799.

[26] P.K. Katti, M.M. Chaudhri, J. Chem. Eng. Data 9 (1964) 442.

[27] M.A. Hernandez-Galvan, F. Garcia-Sanchez, R. Macias-Salinas, Fluid Phase Equilib., 262 (2007) 51.

[28] M.H. Cohen, D. Turnbull, J. Chem. Phys., 31 (1959) 1164.

[29] G.C. Benson, O.K. Kiyohara, J. Chem. Thermodyn., 11 (1979) 1061.

[30] W.E. Acree, J. Chem. Eng. Data 28 (1983) 215.

[31] C.B. Salguero, J.G. Fadrique, J. Chem. Eng. Data 56 (2011) 3823.

[32] J.M. Resa, J.M. Goenaga, A.I. Sa´nchez-Ruiz, J. Chem. Eng. Data 51 (2006) 1294.

[33] D.L. Cunha, J.A.P. Coutinho, J.L. Daridon, R.A. Reis, M.L.L. Paredes, J. Chem. Eng. Data 58 (2013) 925.

[34] S. Nallani, S. Boodida, S.J. Tangeda, J. Chem. Eng. Data 52 (2007) 405.

[35] M.S. Dhillon, H.S. Chugh, J. Chem. Eng. Data 22 (1977) 262.

[36] M.I. Aralaguppi, C.V. Jadar, T.M. Aminabhavi, J. Chem. Eng. Data 44 (1999) 441.

[37] A. Ali, A.K. Nain, D. Chand, R. Ahmad, J. Chinese. Chem. Soc., 53 (2006) 531.

[38] J.R. Partington, *An Advanced Treatise on Physical Chemistry*, Longmans & Green, London, 1953, Vol.4, Sec X.

[39] P.D. Vaz, P.J.A.R-. Claro, J. Raman. Spectros., 34 (2003) 863.

[40] H. Yamada, Bull. Chem. Soc. Jpn., 32 (1959) 1051.